



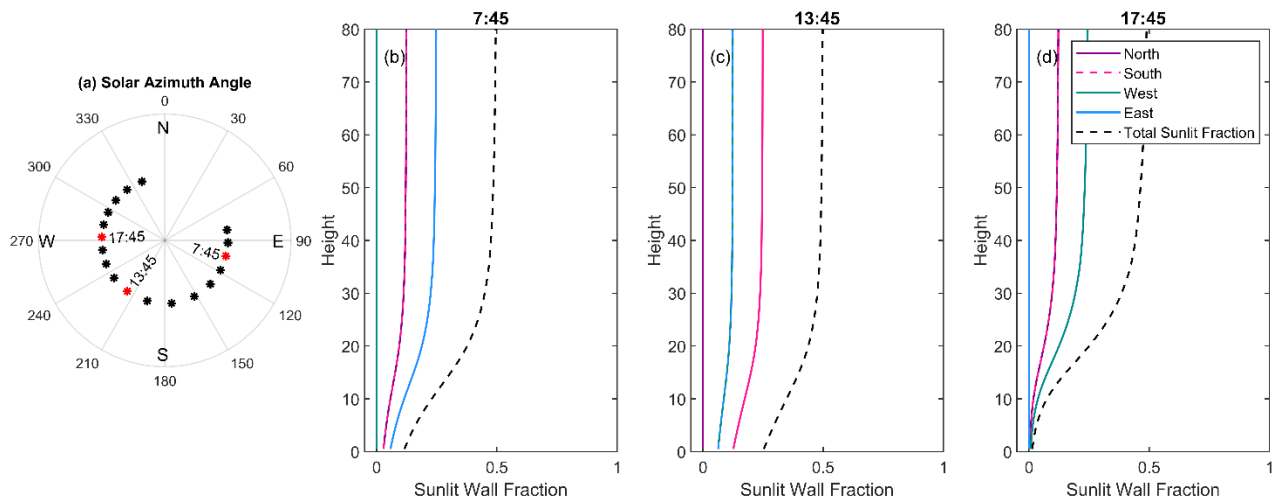
*Supplement of*

## **Evaluation of vertically resolved longwave radiation in SPARTACUS-Urban 0.7.3 and the sensitivity to urban surface temperatures**

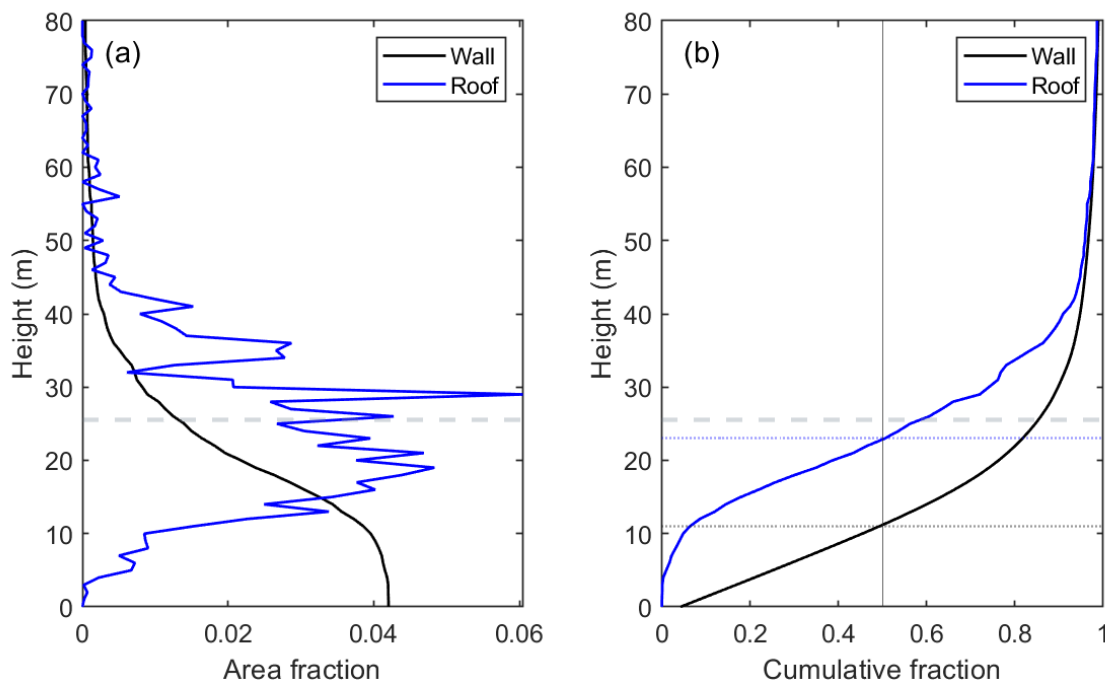
**Megan A. Stretton et al.**

*Correspondence to:* Megan A. Stretton ([m.a.stretton@reading.ac.uk](mailto:m.a.stretton@reading.ac.uk))

The copyright of individual parts of the supplement might differ from the article licence.



5 **Figure S1:** Demonstration of the  $T_{wall}$  averaging method used for SPARTACUS-Urban simulations (Section 3.3). Wall types are weighted using (a) solar azimuth angle for each time as in Eq. 4 and Eq. 5, resulting in (b-d) sunlit fraction profiles for each time step that are used to weight the sunlit-shaded temperatures (Figure 3) to determine profiles in Figure 5. Red scatter in (a) shows azimuth angle of times used in further panels.



10 **Figure S2:** Vertical profiles for a 2 km  $\times$  2 km domain in central London of (a) fractional wall (black) and roof (blue) area and (b) cumulative fraction. Dashed grey lines denote the mean building height. Dotted blue and grey lines show the heights where cumulative fraction reaches 50%.

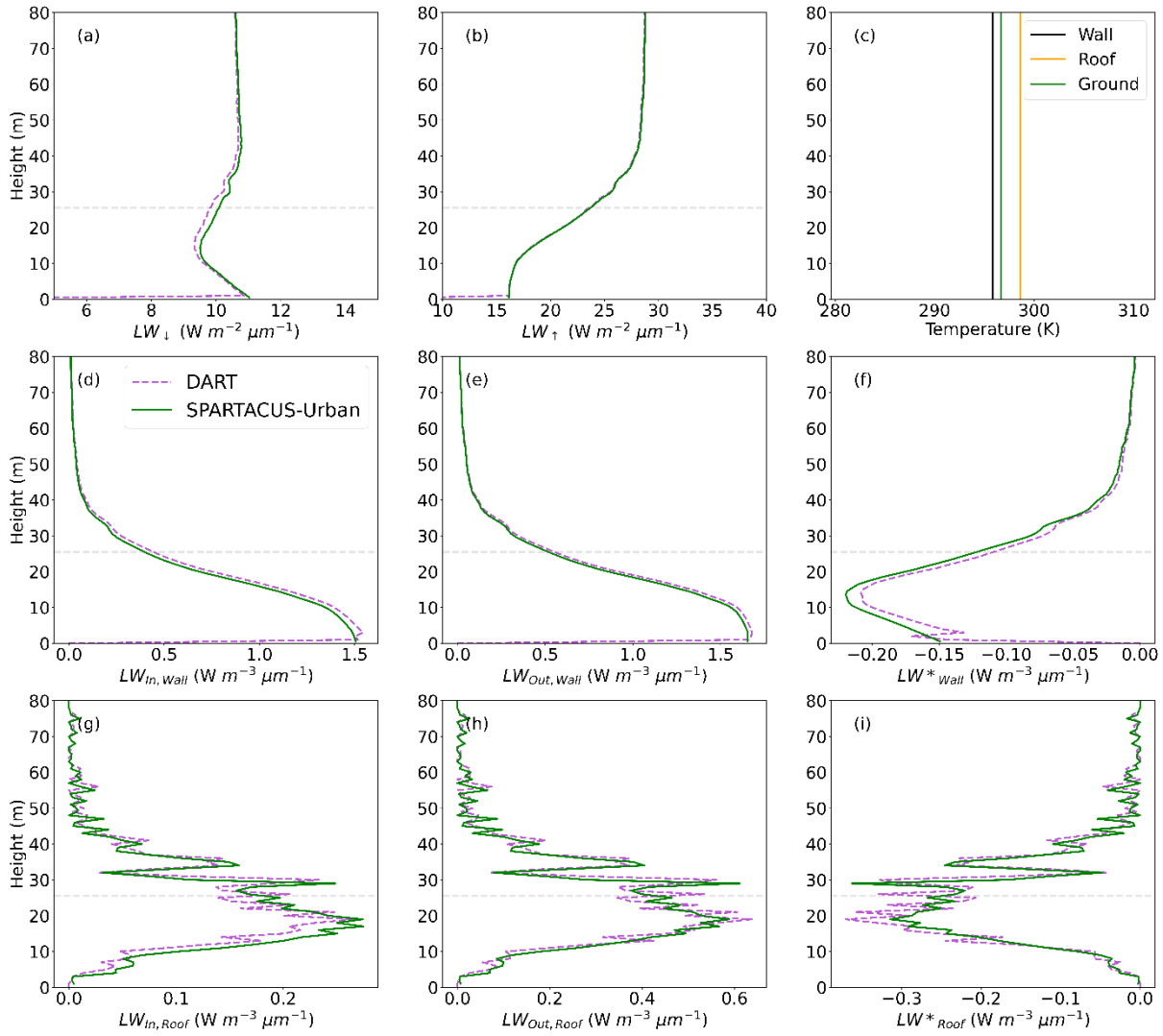
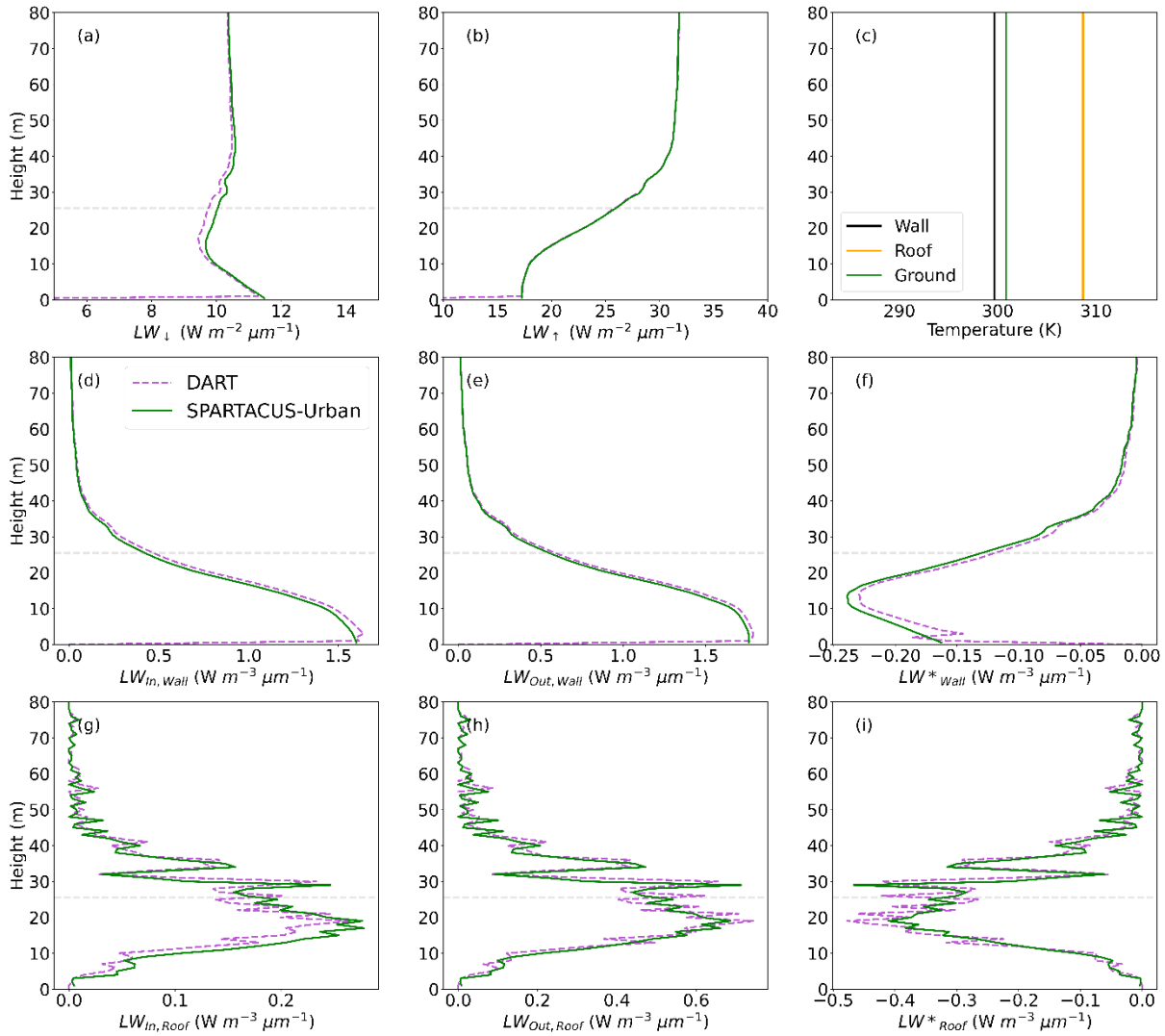
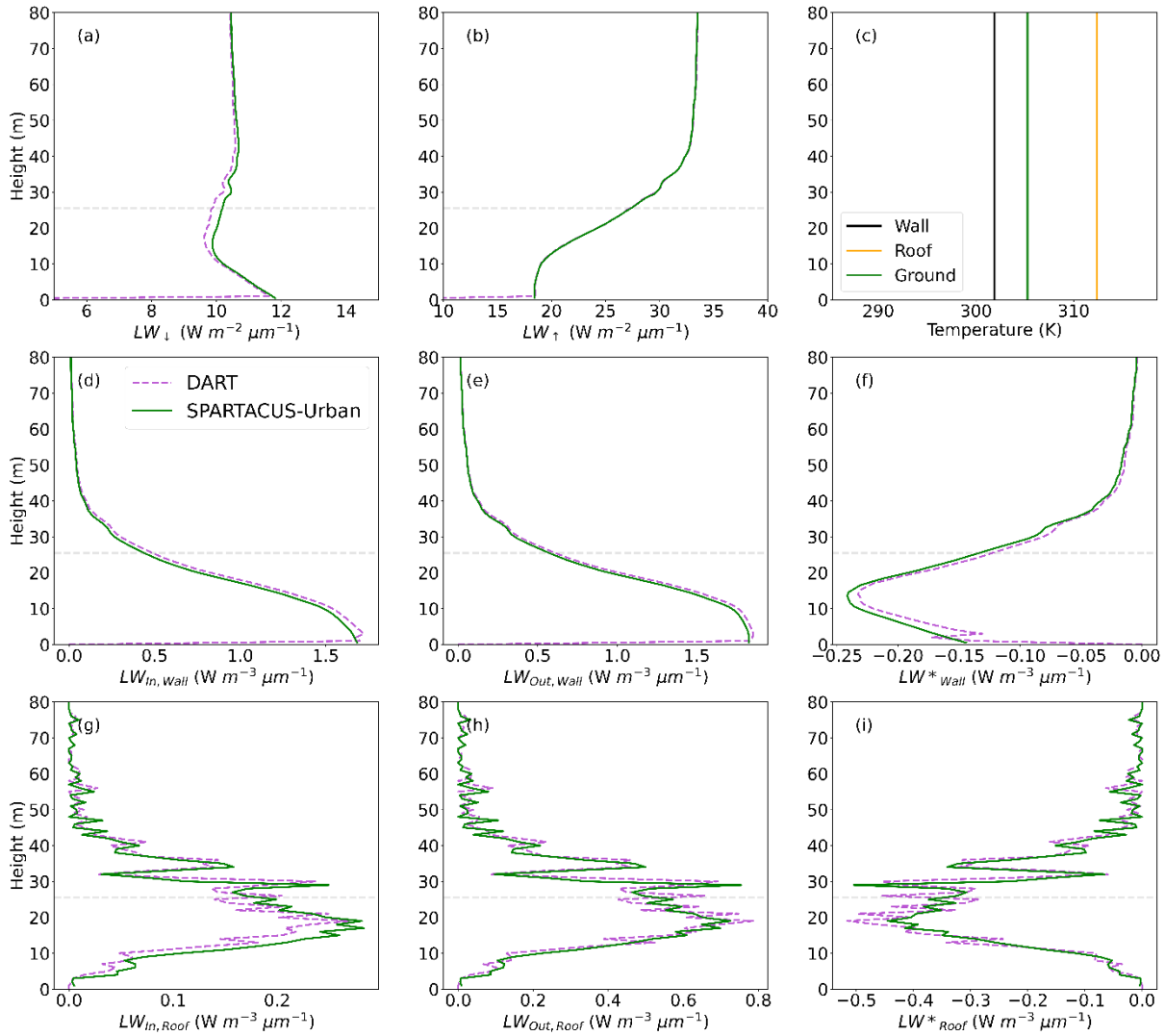


**Figure S3:** Longwave fluxes (LW) for a  $2 \text{ km} \times 2 \text{ km}$  domain in central London (Figure 1) simulated with SPARTACUS-Urban (green) and DART (purple) with an emissivity of 0.93 at 7:45 UTC on the 27<sup>th</sup> August 2017 with (c) single facet T: (a) downwelling clear air flux ( $LW_{\downarrow}$ ), (b) upwelling clear air flux ( $LW_{\uparrow}$ ), (d-f) wall interception, outgoing and net flux ( $LW_{In,Wall}$ ,  $LW_{Out,Wall}$ ,  $LW^*_{Wall}$ ), (g-i) roof interception, outgoing and net flux ( $LW_{In,Roof}$ ,  $LW_{Out,Roof}$ ,  $LW^*_{Roof}$ ). Prescribed facet temperatures using: a single temperature per surface type for DART, and (c) single temperatures per facet type for SPARTACUS-Urban.

15



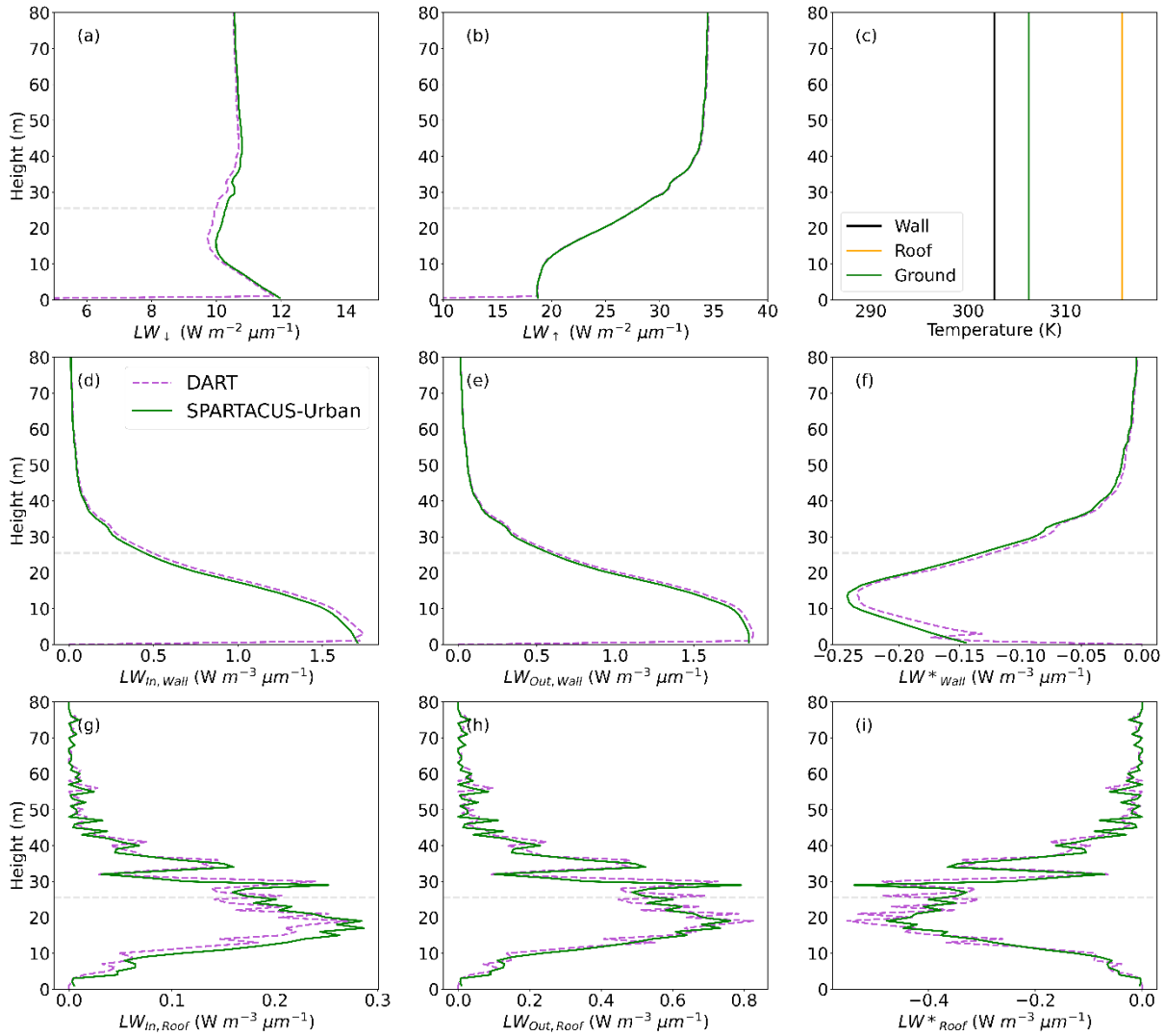
20 **Figure S4:** Longwave fluxes (LW) for a  $2 \text{ km} \times 2 \text{ km}$  domain in central London (Figure 1) simulated with SPARTACUS-Urban (green) and DART (purple) with an emissivity of 0.93 at 9:45 UTC on the 27<sup>th</sup> August 2017 with (c) single facet T: (a) downwelling clear air flux ( $LW_{\downarrow}$ ), (b) upwelling clear air flux ( $LW_{\uparrow}$ ), (d-f) wall interception, outgoing and net flux ( $LW_{In,Wall}$ ,  $LW_{Out,Wall}$ ,  $LW^*_{Wall}$ ), (g-i) roof interception, outgoing and net flux ( $LW_{In,Roof}$ ,  $LW_{Out,Roof}$ ,  $LW^*_{Roof}$ ). Prescribed facet temperatures using: a single temperature per surface type for DART, and (c) single temperatures per facet type for SPARTACUS-Urban.



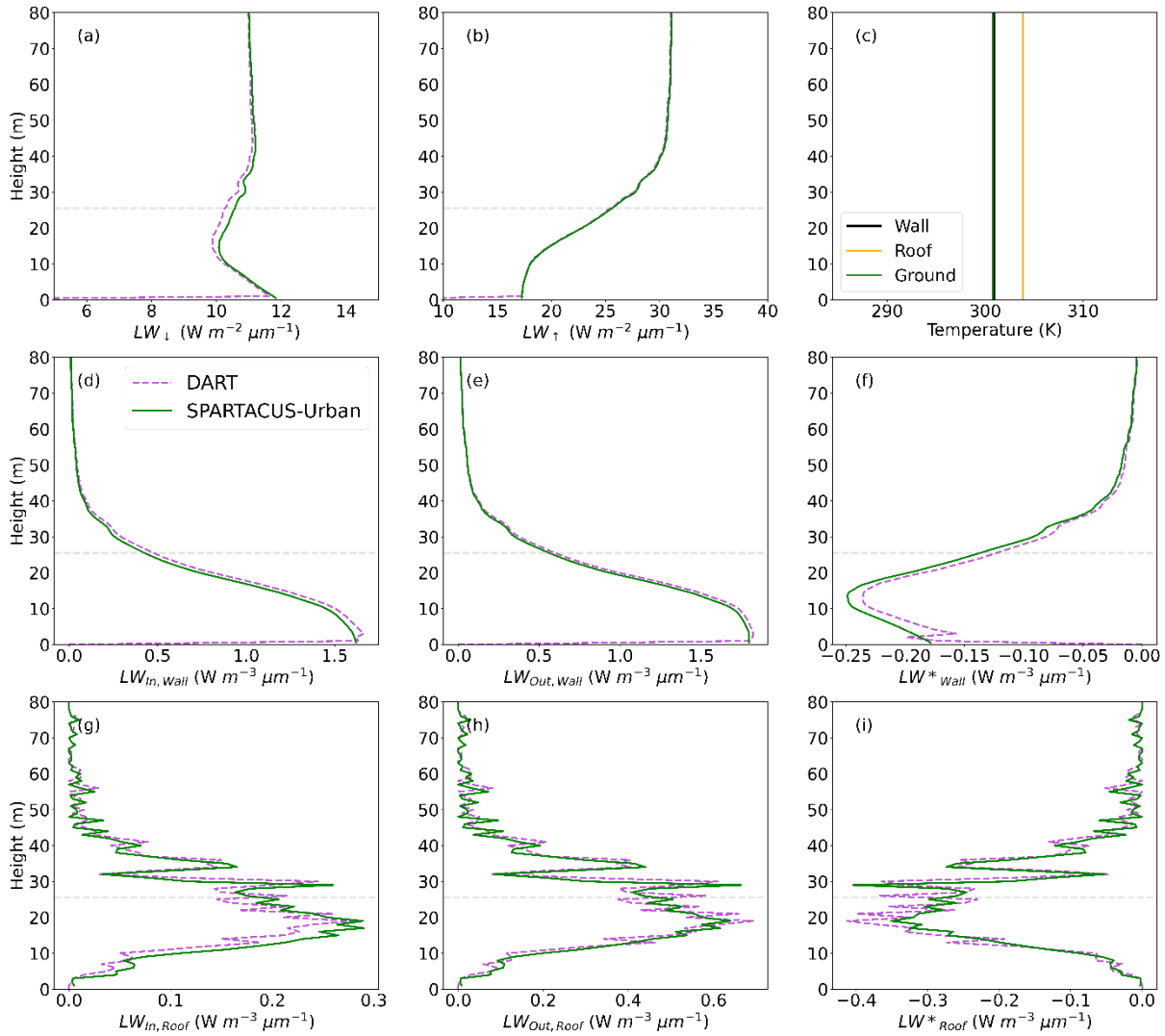
25

**Figure S5:** Longwave fluxes (LW) for a  $2 \text{ km} \times 2 \text{ km}$  domain in central London (Figure 1) simulated with SPARTACUS-Urban (green) and DART (purple) with an emissivity of 0.93 at 11:45 UTC on the 27<sup>th</sup> August 2017 with (c) single facet T: (a) downwelling clear air flux ( $LW_{\downarrow}$ ), (b) upwelling clear air flux ( $LW_{\uparrow}$ ), (d-f) wall interception, outgoing and net flux ( $LW_{In,Wall}$ ,  $LW_{Out,Wall}$ ,  $LW^*_{Wall}$ ), (g-i) roof interception, outgoing and net flux ( $LW_{In,Roof}$ ,  $LW_{Out,Roof}$ ,  $LW^*_{Roof}$ ). Prescribed facet temperatures using: a single temperature per surface type for DART, and (c) single temperatures per facet type for SPARTACUS-Urban.

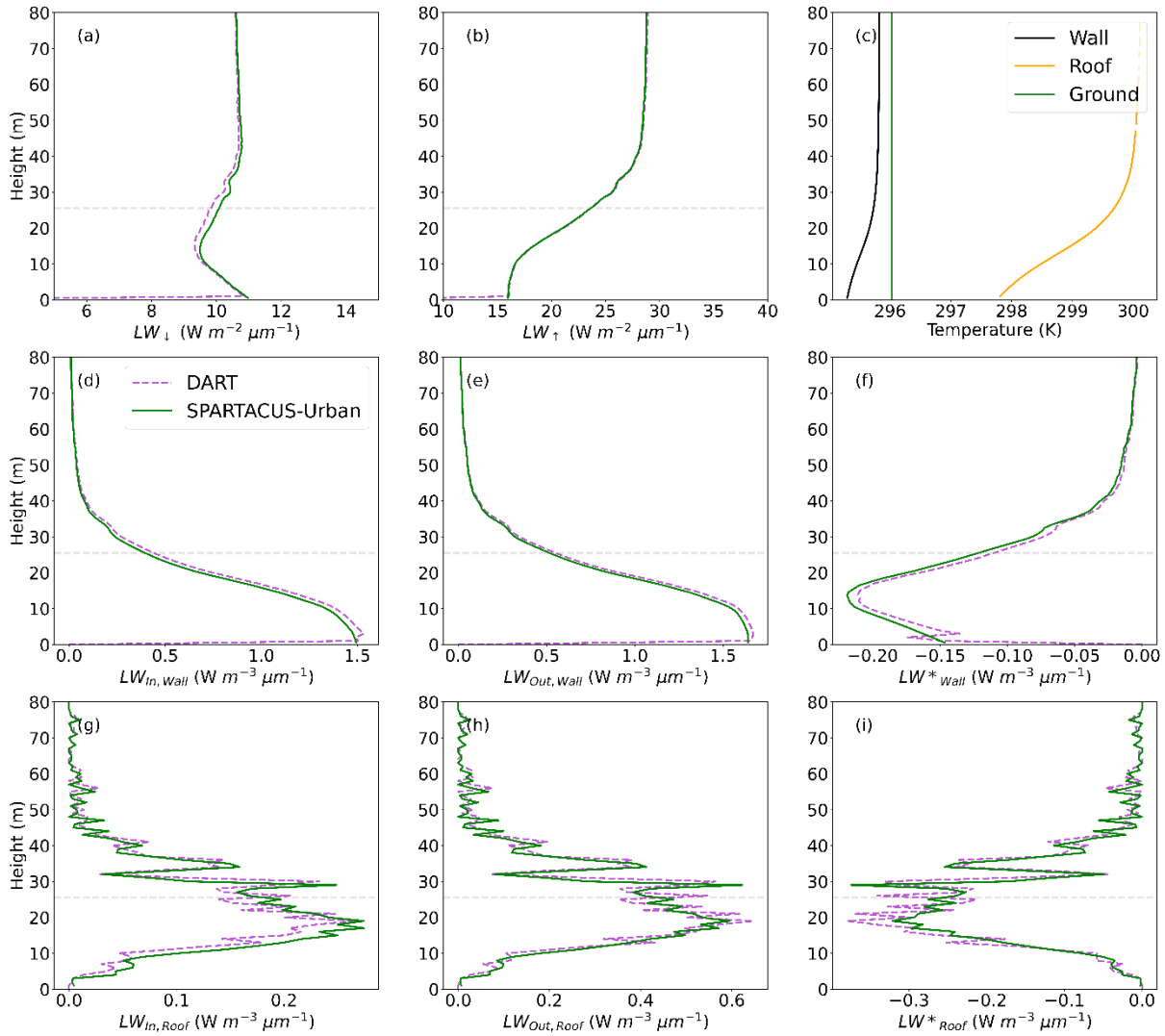
30



35 **Figure S6:** Longwave fluxes (LW) for a  $2 \text{ km} \times 2 \text{ km}$  domain in central London (Figure 1) simulated with SPARTACUS-Urban (green) and DART (purple) with an emissivity of 0.93 at 13:45 UTC on the 27<sup>th</sup> August 2017 with (c) single facet T: (a) downwelling clear air flux ( $LW_{\downarrow}$ ), (b) upwelling clear air flux ( $LW_{\uparrow}$ ), (d-f) wall interception, outgoing and net flux ( $LW_{In,Wall}$ ,  $LW_{Out,Wall}$ ,  $LW^*_{Wall}$ ), (g-i) roof interception, outgoing and net flux ( $LW_{In,Roof}$ ,  $LW_{Out,Roof}$ ,  $LW^*_{Roof}$ ). Prescribed facet temperatures using: a single temperature per surface type for DART, and (c) single temperatures per facet type for SPARTACUS-Urban.

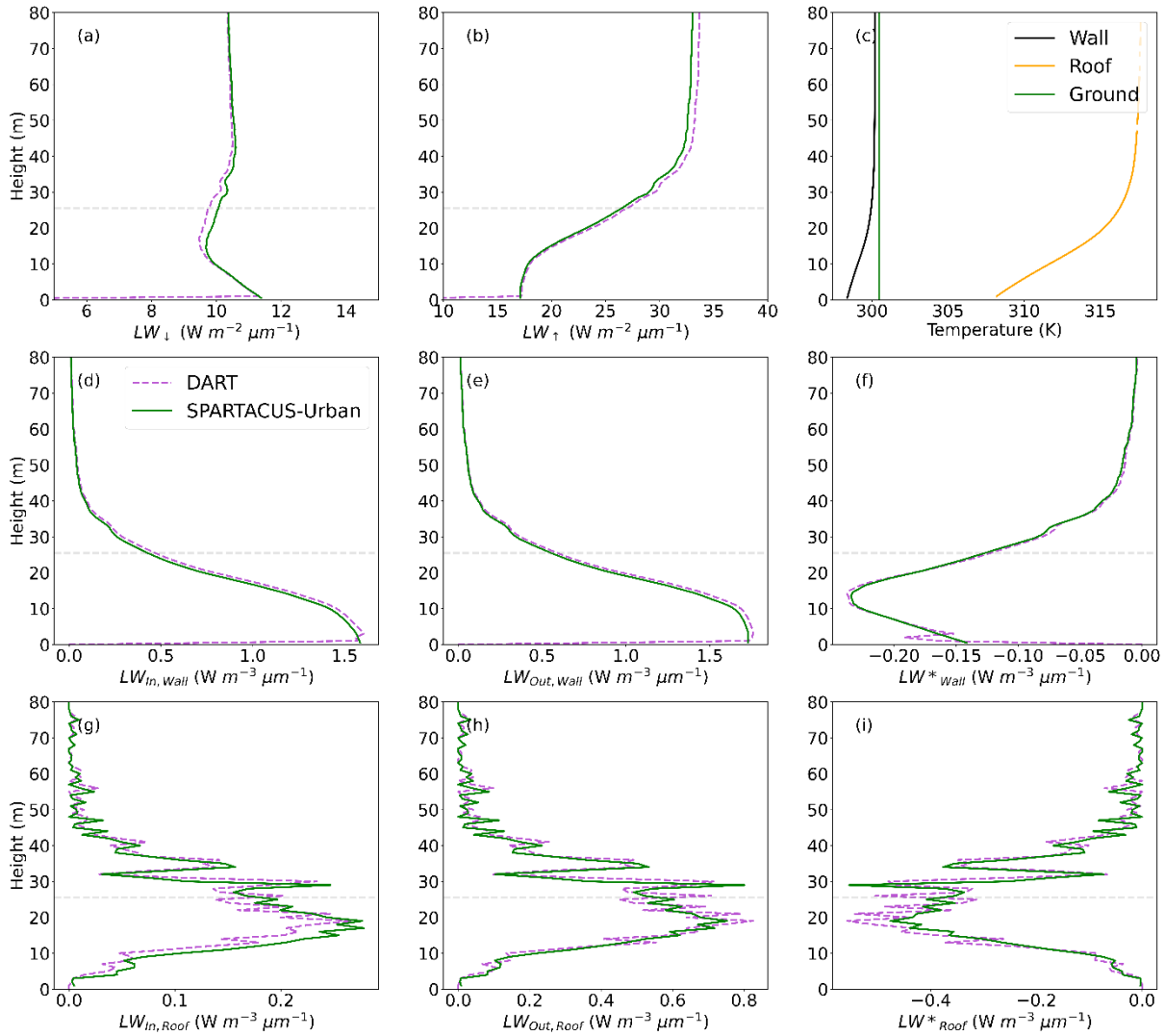


40 **Figure S7:** Longwave fluxes (LW) for a  $2 \text{ km} \times 2 \text{ km}$  domain in central London (Figure 1) simulated with SPARTACUS-Urban (green) and DART (purple) with an emissivity of 0.93 at 17:45 UTC on the 27<sup>th</sup> August 2017 with (c) single facet T: (a) downwelling clear air flux ( $LW_{\downarrow}$ ), (b) upwelling clear air flux ( $LW_{\uparrow}$ ), (d-f) wall interception, outgoing and net flux ( $LW_{In,Wall}$ ,  $LW_{Out,Wall}$ ,  $LW^*_{Wall}$ ), (g-i) roof interception, outgoing and net flux ( $LW_{In,Roof}$ ,  $LW_{Out,Roof}$ ,  $LW^*_{Roof}$ ). Prescribed facet temperatures using: a single temperature per surface type for DART, and (c) single temperatures per facet type for SPARTACUS-Urban.

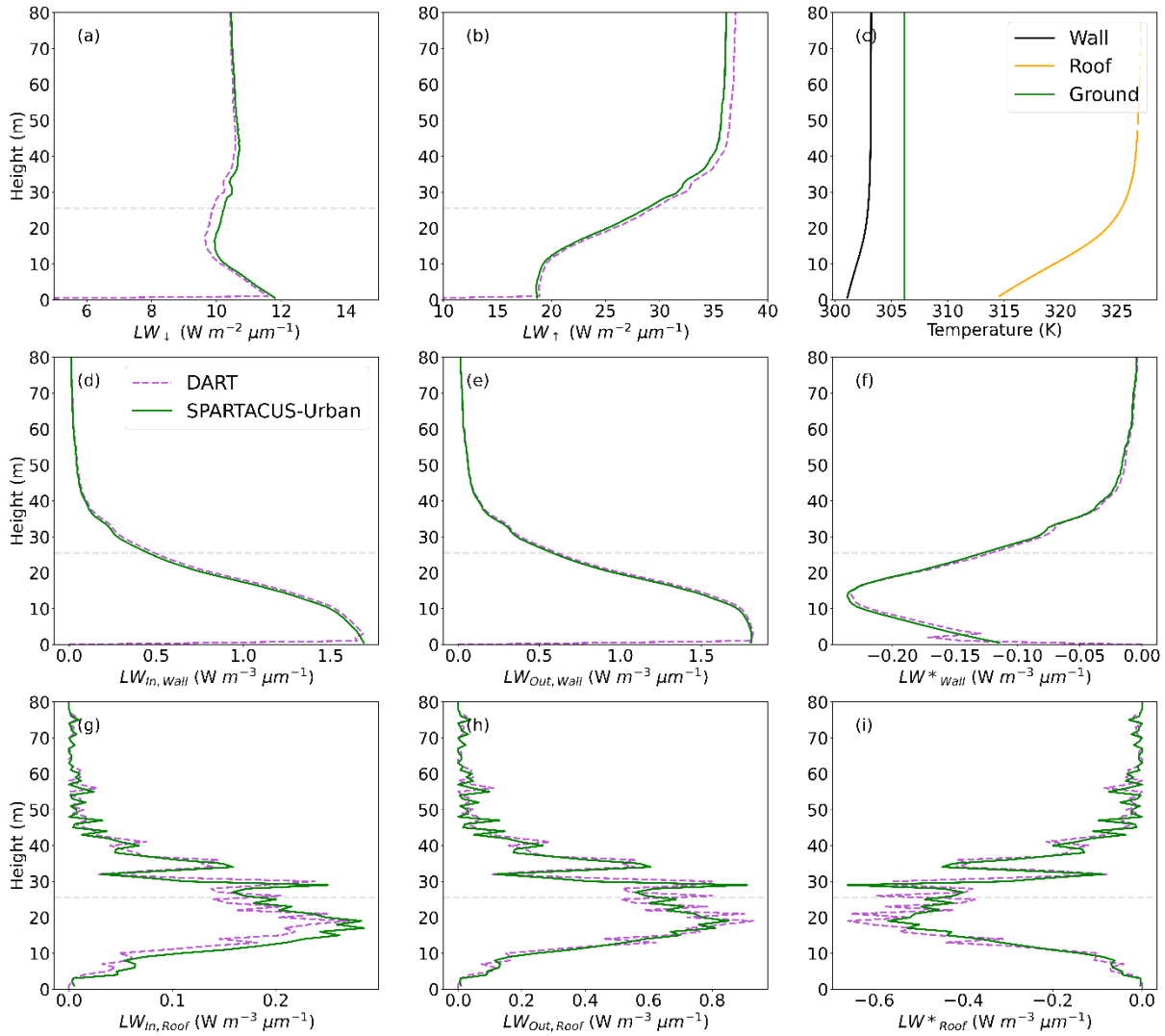


**Figure S8:** Longwave fluxes (LW) for a 2 km x 2 km domain in central London (Figure 1) simulated with SPARTACUS-Urban (green) and DART (purple) with an emissivity of 0.93 at 7:45 UTC on the 27<sup>th</sup> August 2017: **(a)** downwelling clear air flux ( $LW_{\downarrow}$ ), **(b)** upwelling clear air flux ( $LW_{\uparrow}$ ), **(d-f)** wall interception, outgoing and net flux ( $LW_{In,Wall}$ ,  $LW_{Out,Wall}$ ,  $LW^*_{Wall}$ ), **(g-i)** roof interception, outgoing and net flux ( $LW_{In,Roof}$ ,  $LW_{Out,Roof}$ ,  $LW^*_{Roof}$ ). Prescribed facet temperatures based on SW simulations at 7:45 using: a full 3D temperature field for DART, and **(c)** temperature profiles per facet type for SPARTACUS-Urban.

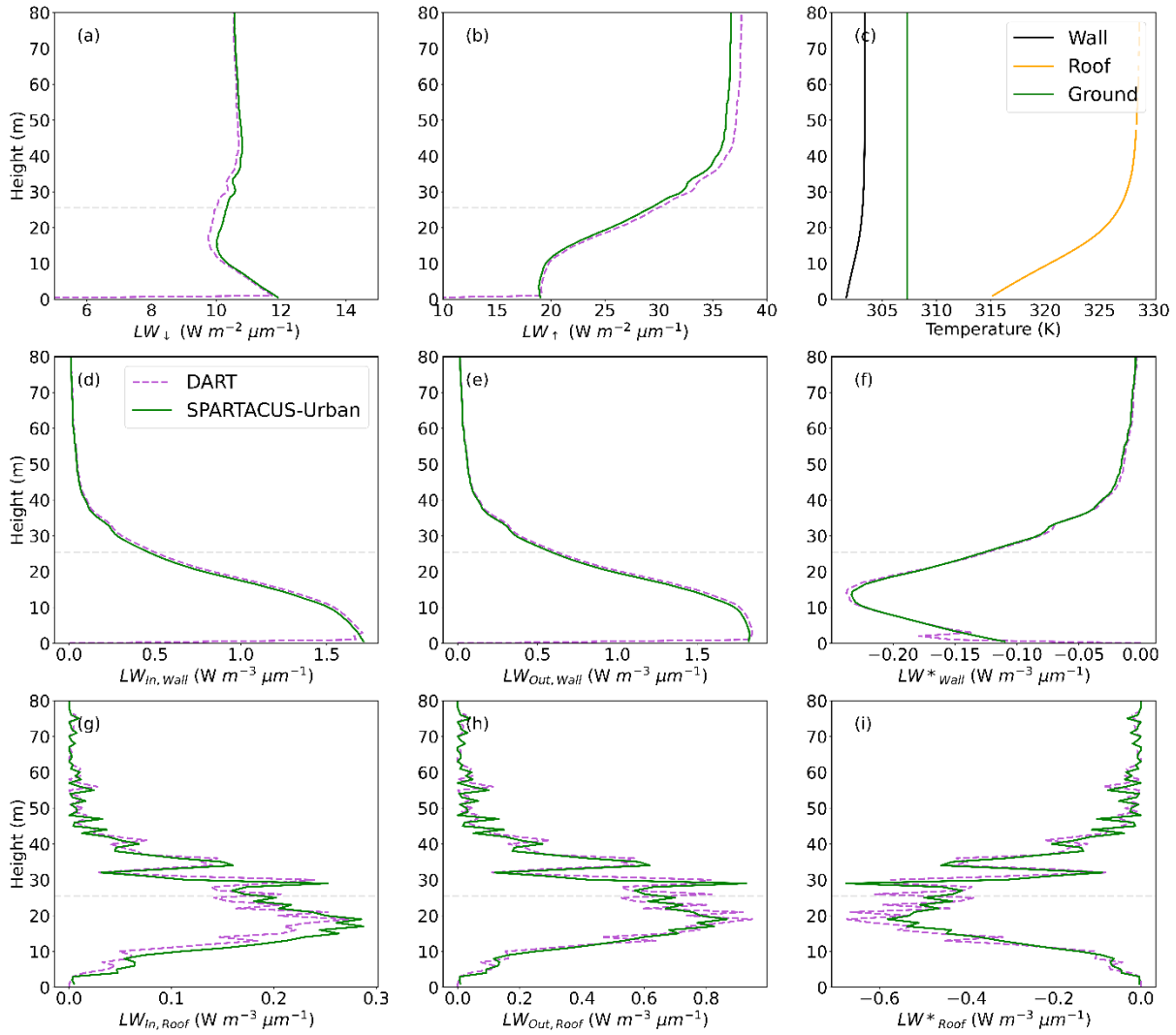
50



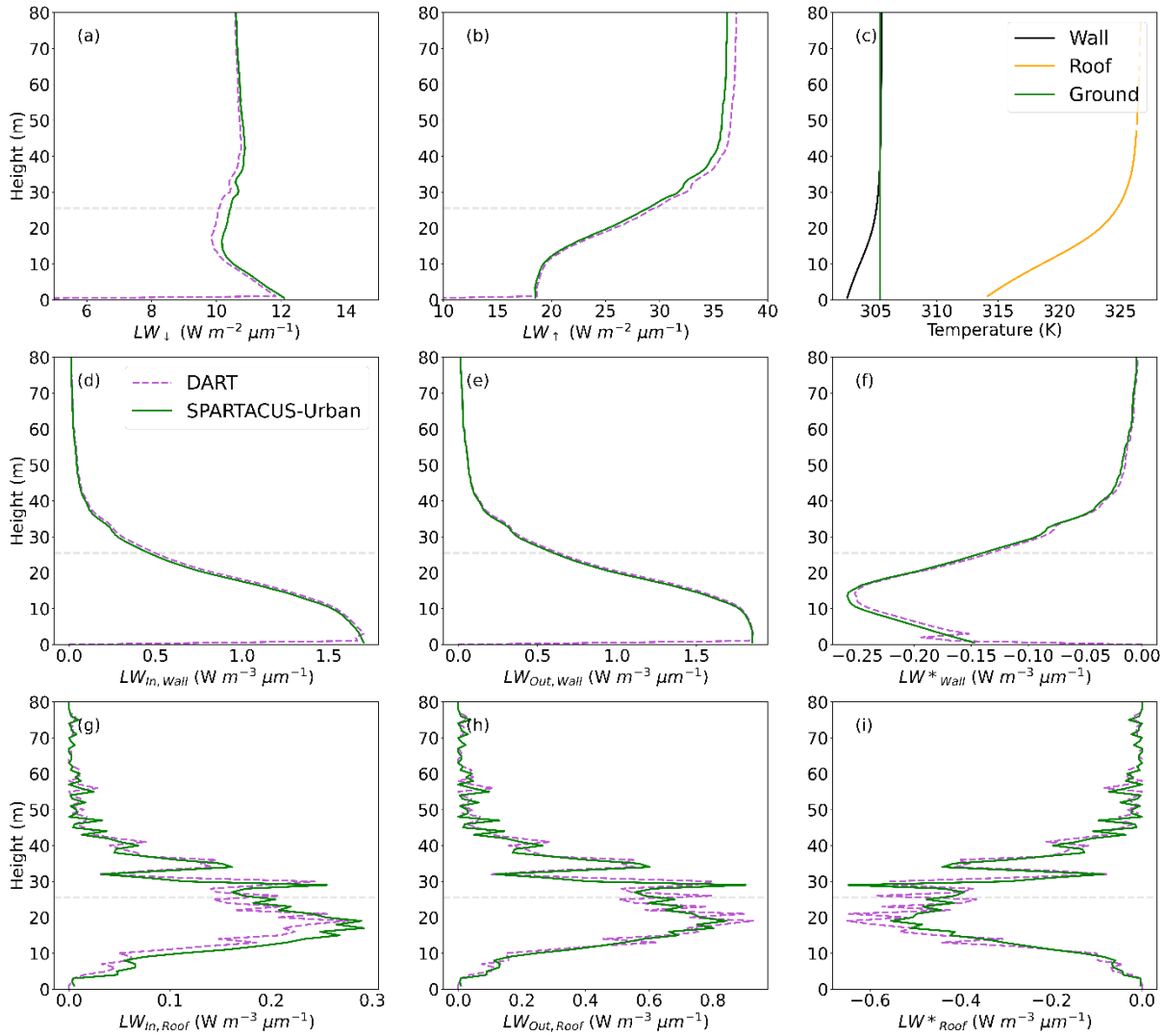
**Figure S9:** Longwave fluxes (LW) for a 2 km x 2 km domain in central London (Figure 1) simulated with SPARTACUS-Urban (green) and DART (purple) with an emissivity of 0.93 at 9:45 UTC on the 27<sup>th</sup> August 2017: (a) downwelling clear air flux ( $LW_{\downarrow}$ ), (b) upwelling clear air flux ( $LW_{\uparrow}$ ), (d-f) wall interception, outgoing and net flux ( $LW_{In,Wall}$ ,  $LW_{Out,Wall}$ ,  $LW^*_{Wall}$ ), (g-i) roof interception, outgoing and net flux ( $LW_{In,Roof}$ ,  $LW_{Out,Roof}$ ,  $LW^*_{Roof}$ ). Prescribed facet temperatures based on SW simulations at 9:45 using: a full 3D temperature field for DART, and (c) temperature profiles per facet type for SPARTACUS-Urban.



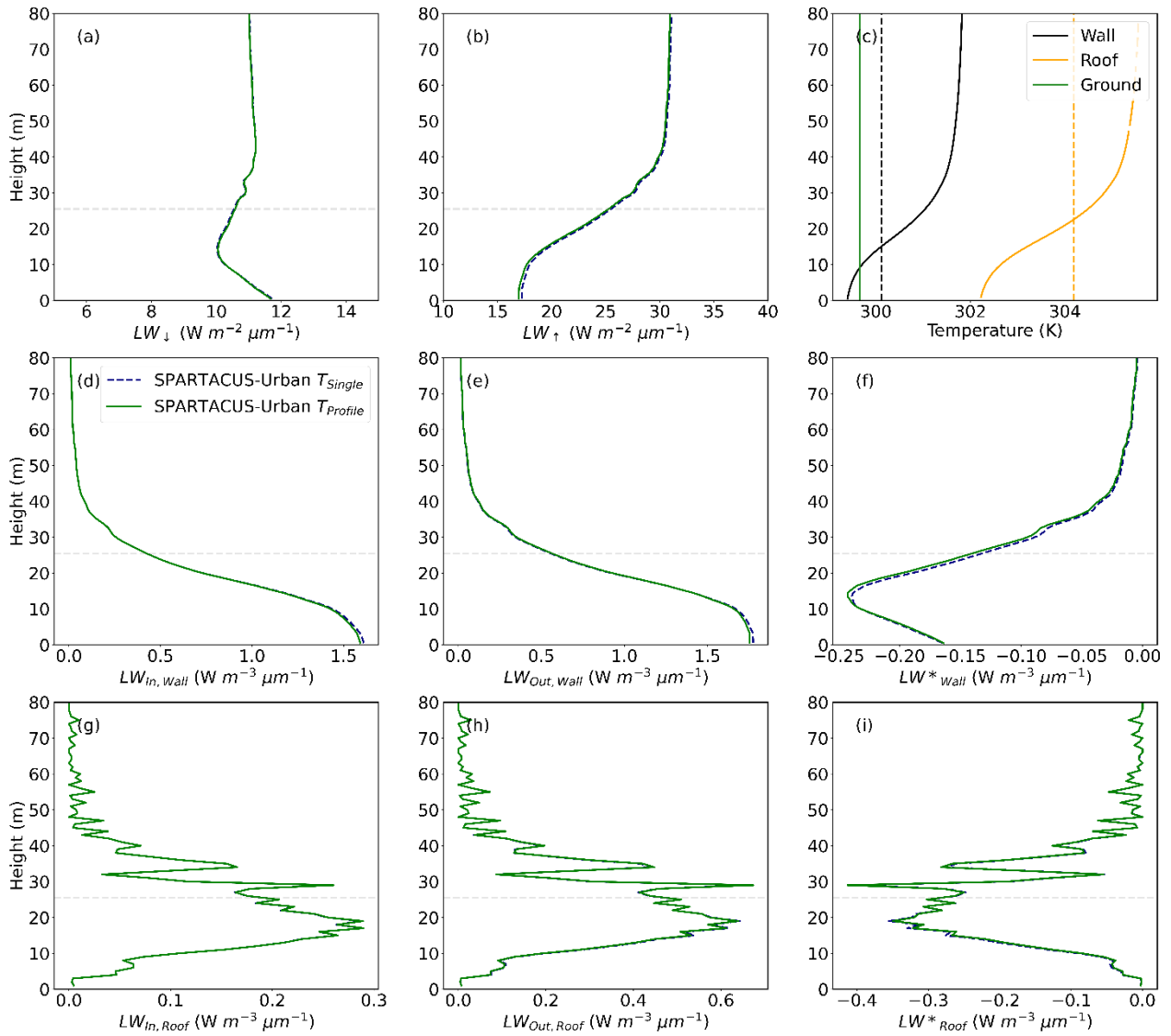
**Figure S10:** Longwave fluxes (LW) for a 2 km x 2 km domain in central London (Figure 1) simulated with SPARTACUS-Urban (green) and DART (purple) with an emissivity of 0.93 at 11:45 UTC on the 27<sup>th</sup> August 2017: (a) downwelling clear air flux ( $LW_{\downarrow}$ ), (b) upwelling clear air flux ( $LW_{\uparrow}$ ), (d-f) wall interception, outgoing and net flux ( $LW_{In,Wall}$ ,  $LW_{Out,Wall}$ ,  $LW^*_{Wall}$ ), (g-i) roof interception, outgoing and net flux ( $LW_{In,Roof}$ ,  $LW_{Out,Roof}$ ,  $LW^*_{Roof}$ ). Prescribed facet temperatures based on SW simulations at 11:45 using: a full 3D temperature field for DART, and (c) temperature profiles per facet type for SPARTACUS-Urban.



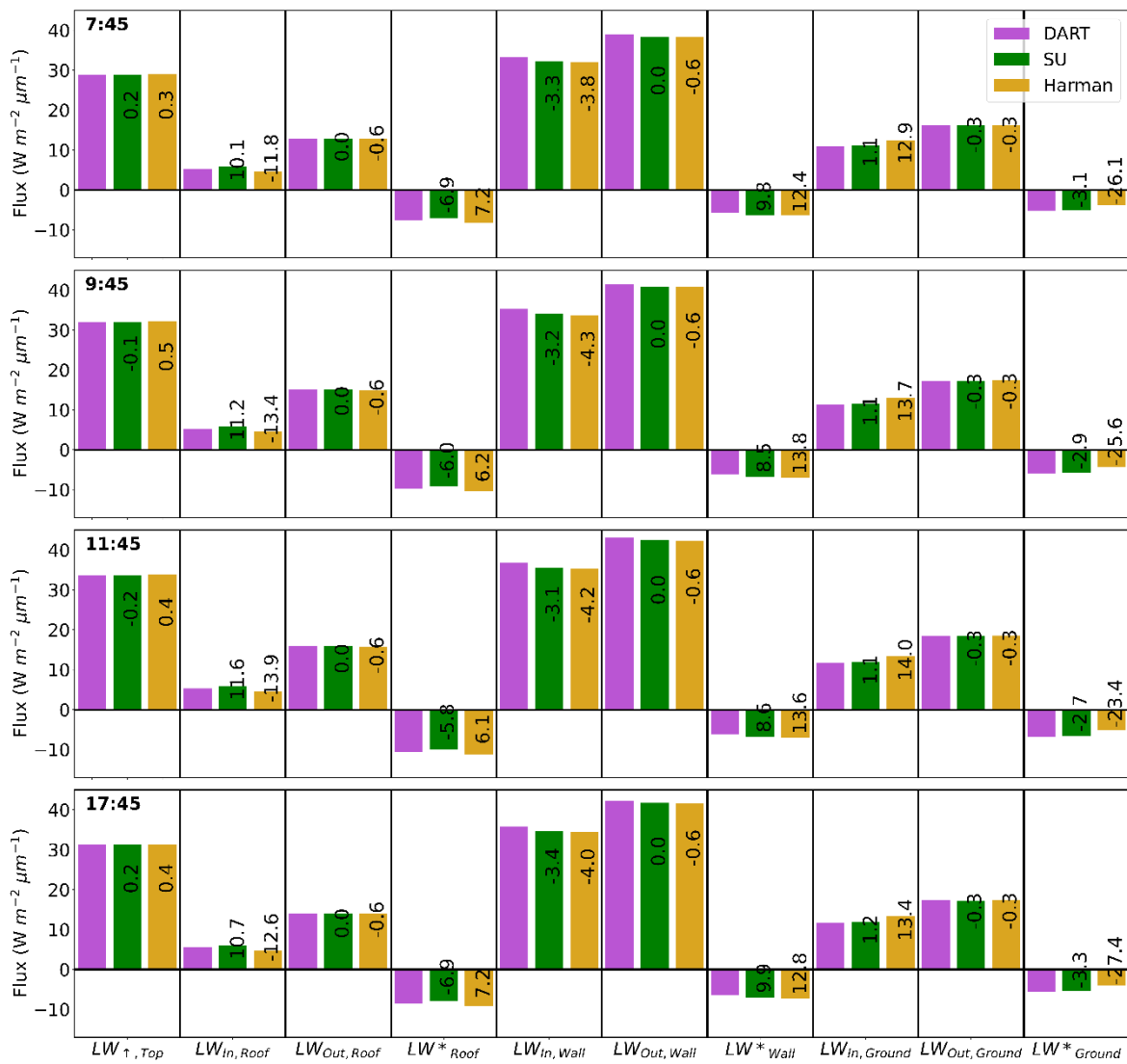
**Figure S11:** Longwave fluxes (LW) for a 2 km x 2 km domain in central London (Figure 1) simulated with SPARTACUS-Urban (green) and DART (purple) with an emissivity of 0.93 at 12:45 UTC on the 27<sup>th</sup> August 2017: **(a)** downwelling clear air flux ( $LW_{\downarrow}$ ), **(b)** upwelling clear air flux ( $LW_{\uparrow}$ ), **(d-f)** wall interception, outgoing and net flux ( $LW_{In,Wall}$ ,  $LW_{Out,Wall}$ ,  $LW^*_{Wall}$ ), **(g-i)** roof interception, outgoing and net flux ( $LW_{In,Roof}$ ,  $LW_{Out,Roof}$ ,  $LW^*_{Roof}$ ). Prescribed facet temperatures based on SW simulations at 12:45 using: a full 3D temperature field for DART, and **(c)** temperature profiles per facet type for SPARTACUS-Urban.



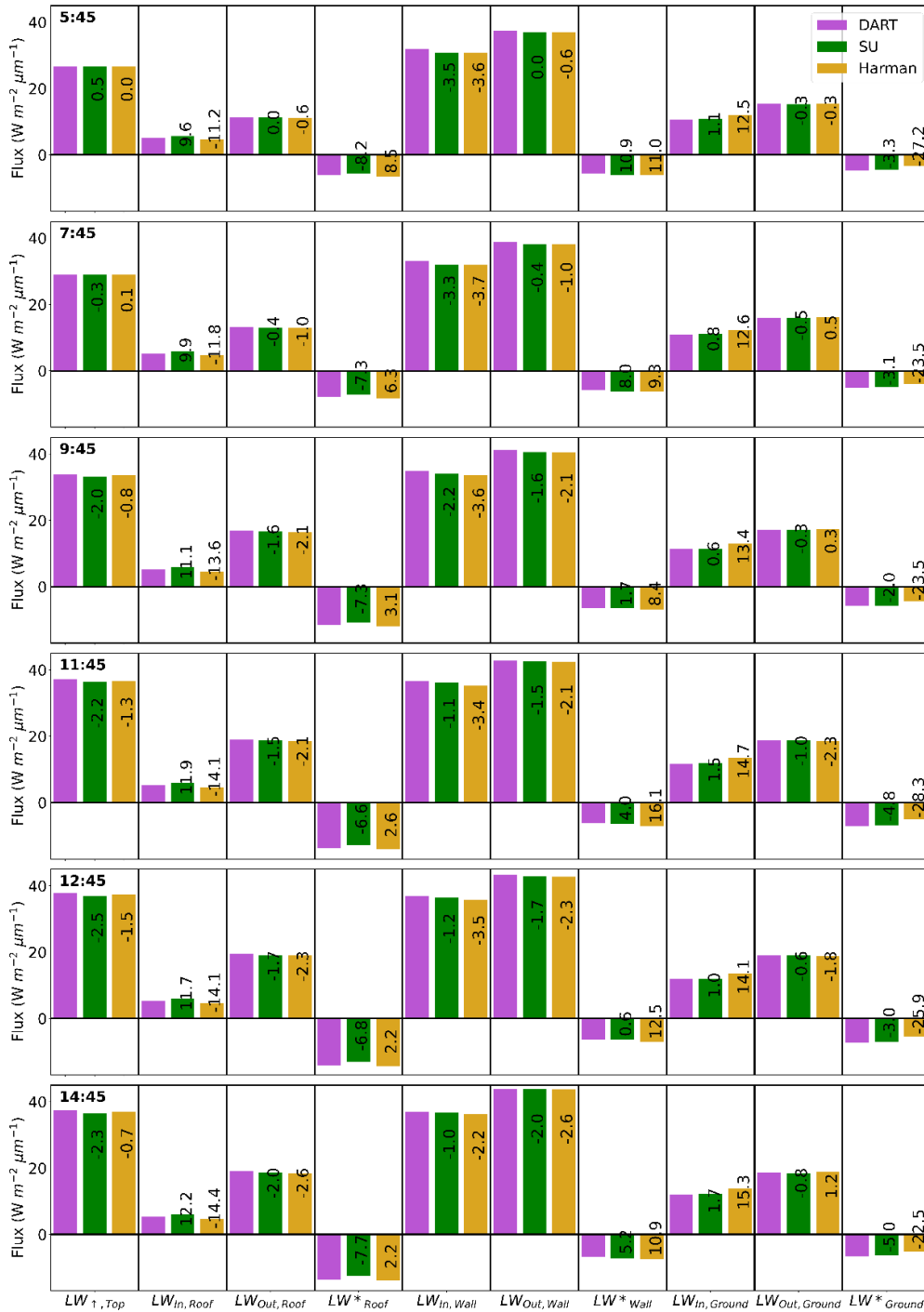
**Figure S12:** Longwave fluxes (LW) for a 2 km x 2 km domain in central London (Figure 1) simulated with SPARTACUS-Urban (green) and DART (purple) with an emissivity of 0.93 at 14:45 UTC on the 27<sup>th</sup> August 2017: (a) downwelling clear air flux ( $LW_{\downarrow}$ ), (b) upwelling clear air flux ( $LW_{\uparrow}$ ), (d-f) wall interception, outgoing and net flux ( $LW_{In,Wall}$ ,  $LW_{Out,Wall}$ ,  $LW^*_{Wall}$ ), (g-i) roof interception, outgoing and net flux ( $LW_{In,Roof}$ ,  $LW_{Out,Roof}$ ,  $LW^*_{Roof}$ ). Prescribed facet temperatures based on SW simulations at 14:45 using: a full 3D temperature field for DART, and (c) temperature profiles per facet type for SPARTACUS-Urban.



**Figure S13:** Longwave (LW) SPARTACUS-Urban simulations for a  $2 \text{ km} \times 2 \text{ km}$  domain in central London (Figure 1) with an emissivity of 0.93 for 17:45 UTC on the 27th August 2017 for: (a) downwelling clear air flux ( $LW_{\downarrow}$ ), (b) upwelling clear air flux ( $LW_{\uparrow}$ ), (d-f) wall interception, outgoing and net flux ( $LW_{In,Wall}$ ,  $LW_{Out,Wall}$ ,  $LW^*_{Wall}$ ), (g-i) roof interception, outgoing and net flux ( $LW_{In,Roof}$ ,  $LW_{Out,Roof}$ ,  $LW^*_{Roof}$ ). Facet temperatures prescribed are (c) a single temperature per facet ( $T_{Single}$ , black dashed) and using temperature profiles for each facet type ( $T_{Profile}$ , green).



60 **Figure S14:** Comparison of simulations for one grid-cell in central London on 27th August at four times (rows, UTC) using nBE (values, Eq. 8) relative to realistic world DART, for SPARTACUS-Urban (SU) and Harman et al. (2004) longwave fluxes with isothermal facet temperatures (Sect. 3.3): upwelling clear air flux at the top of the canopy ( $LW_{\uparrow}$ ), and the roof, wall, and ground total interception, outgoing, and net flux.



65 **Figure S15:** Comparison of simulations for one grid-cell in central London on 27th August at six times (rows, UTC) using nBE (values, Eq. 8) relative to realistic world DART, for SPARTACUS-Urban (SU) and Harman et al. (2004) longwave fluxes with facet temperatures prescribed based on SW simulations (Sect. 3.3), upwelling clear air flux at the top of the canopy ( $LW_{\uparrow}$ ), and the roof, wall, and ground total interception, outgoing, and net flux.